



A DAMPER-SPRING DEVICE FOR SEISMIC ENERGY DISSIPATION IN BUILDINGS

F. Hernández⁽¹⁾, R. Astroza⁽²⁾, J.F. Beltrán⁽³⁾, L. Belmar⁽⁴⁾

⁽¹⁾ Assistant Professor, Department of Civil Engineering, Universidad de Chile, fhernandezp@ing.uchile.cl

⁽²⁾ Assistant Professor, Faculty of Engineering and Applied Sciences, Universidad de los Andes, raastroza@miuandes.cl

⁽³⁾ Associate Professor, Department of Civil Engineering, Universidad de Chile, ibeltran@ing.uchile.cl

⁽⁴⁾ Civil Engineer, Department of Civil Engineering, Universidad de Chile, leobelmarv@gmail.com

Abstract

A damper-spring energy dissipation device connected in series with a cable that is extended throughout the entire structure by an array of pulleys is proposed, which is experimentally tested and validated on a reduced-scale five-story shear building. A series of seismic tests conducted on a shake table show that the proposed system concentrates the inter-story drifts experienced throughout the height of the structure in the proposed damper-spring; therefore, a unique spring-damper system can reduce the seismic response significantly, by increasing the damping ratios of all the structural modes. Different dynamic response quantities are mitigated, including the inter-story drifts, which decrease by about 70% compared to those experienced by the structure without the proposed dissipation system. It is also shown that the proposed scheme provides an energy dissipation capacity comparable to that offered by placing one damper on every floor, confirming the efficiency of this novel device. The system exhibits a significant nonlinear response evidenced by the variations of the natural frequencies and damping ratios of the building during the seismic tests. In particular, the time-variant natural frequencies were identified by using the Short-Time Transfer Function method. Finally, a novel approach is presented and validated that allows determining the time-variant damping ratios and mode shapes of the building by adjusting the model-predicted response with measured absolute acceleration time histories during seismic tests.

Keywords: Damper with cable and pulley system; STTF; time-variant damping ratios; Mod- ζ (var) approach.

1. Introduction

Seismic energy dissipation devices are installed in civil structures to increase the effective damping ratios of civil structures. Therefore, they are employed to reduce structural damage and/or improve the seismic performance, mitigating the damage of nonstructural elements and components. In this context, fluid viscous dampers are commonly used that allow dissipating seismic energy through the flowing of a high viscous fluid through orifices inside the device when the damper is subjected to differential velocities [1].

Stiff structures and tall buildings commonly experience limited inter-story drifts during an earthquake. For example, Lagos et al.[2] have shown that buildings designed following the Chilean design practice, i.e., reinforced concrete (RC) buildings with shear walls, could only experience inter-story drifts ratios no more significant than 0.5%, even during large earthquakes. Therefore, a common practice is to use seismic energy dissipation devices connected between two or three floors in order to accumulate larger deformations into the energy dissipation devices and improve their seismic energy dissipation efficiency. Similarly, some researchers have proposed different techniques to optimize the location of viscous-elastic dampers in a structure in order to maximize their efficiency [3,4] rather than using multiples energy dissipation devices placed on every floor of the structure.



In this research, a novel system consisting of fluid viscous dampers connected in parallel with spring and linked in series with a cable is proposed. The aim is that the cable can concentrate the inter-story deformation of multiple floors of the building by using a spatial arrangement of pulleys throughout the full height of the structure. Thus, the proposed system accumulates the inter-story drifts of all the connected floors allowing dissipate the seismic energy by using only one damper-spring system. The proposed dissipation system has the following advantages: (i) reduces the number of energy dissipation devices to be installed (reducing costs), making the damper-spring a more efficient device; (ii) minimize architecturally invasive since the cable can be hidden behind the façade of the structure, (iii) provides a low additional lateral stiffness to the structure, which is determined by the damper-spring stiffness, and (iv) provide additional energy dissipation through the interaction between the cable and the pulley to the system due to the friction and viscous dissipation generated inside the pulley mechanisms. The proposed system is experimentally tested on a small-scale five-story shear building, which was subjected to multiple pull-backs and seismic tests on a shake table. To verify the effectiveness of the system, the same structure without the additional devices, the structure with dampers on every floor, and the structure only with the cable (i.e., without the damper-spring in series) were also tested. The responses are analyzed in terms of the capability of the proposed system to reduce the inter-story drift and shear forces and to increase the energy dissipation capabilities. Since the structural response when the proposed system is included is non-linear elastic (e.g., self-centering system), the time-variant natural frequencies of the structure are identified using the short time transfer function (STTF) method [5] and a the Mod- ζ (var) method [6].

2. Experimental Setup

A small-scale five-story shear building was mounted on a shake table (Fig. 1). The structure was built with five floors using 5mm thick ASTM A36 steel slabs of 30cm×30cm in dimension. Each floor was supported by four columns, located at each corner with variable story heights (42cm for the top three stories and 35cm for the bottom two stories). The columns were made of 3cm wide by 3mm thick ASTM A36 steel bars, and were connected to the floor plates using bolts and universal semicircular joints. For the energy dissipation system, a 2mm diameter galvanized steel cable (1×19 AA) with an ultimate tensile strength of 3.785kN was employed. Pulleys were attached to the structure using special metal connectors. A 100mm long hydraulic viscous damper was used, which was trimmed from a commercial aluminum shock absorber. The damper-spring system was made by connecting a tensile spring to the damper using two small metal plates. To ensure the system operates when the structure deformed in both directions (i.e., the cable only in tension), pre-tensioning stress was applied to the cable, and the magnitude was determined so that the initial position of the damper was near to the center of its fully extended length (± 2 cm). Two parallel systems were mounted on both sides of the structure in an asymmetric manner to reduce possible asymmetric effects. The small-scale building did not exhibit significant mass and stiffness eccentricities and was orientated to be excited by the shake table along its flexible direction (Fig. 1b). Therefore, the seismic response of the tested structure can be adequately described by a two-dimensional (2D) model.

The structure was instrumented with seven accelerometers (Kistler[®] model K-beam 8304B2) installed at different levels and also at the base (Fig. 1b). The roof level was instrumented with two eccentric accelerometers to monitor the potential torsional response of the building. The data were acquired by using a National Instrument PCI-6229 (16-Bit, 250 kS/s) DAQ at a sampling rate of 400 Hz.

The structure was tested in four different configurations (Fig. 2): Configuration A is a benchmark including the structure itself without any energy dissipators or cable; Configuration B refers to the structure with the spring-damper in series with the cable running throughout the entire structure; Configuration C is associated with the structure and the cable only (without the spring-damper); and Configuration D corresponds to the structure with damper-spring systems placed at every story. The structures were tested under seismic ground accelerations using the shake table. Herein, the results for the strong motion recorded at the Concepcion Centro station during the 2010 M_w 8.8 Maule-Chile Earthquake was used with the amplitude scaled to 50%. It is worth noting that because of the influence of the upper structure, the real inputs to the structures are quite close but do not match perfectly. It is worth noting that the results presented



in the following sections have a common time (i.e., they were synchronized) according to the seismic input motion generated by the shake table. Overall, the response spectrums of the absolute acceleration with a damping ratio of 5% for the different configurations of the structures were very close [6]. Therefore, direct comparisons between responses from different configured structures above can be made.

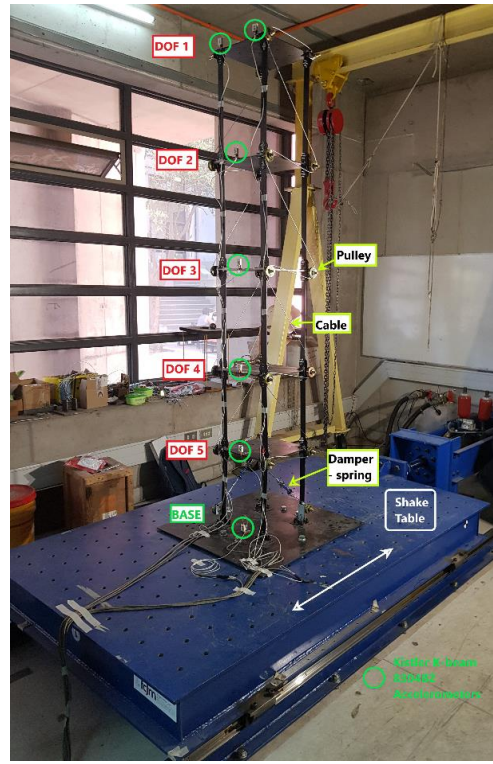
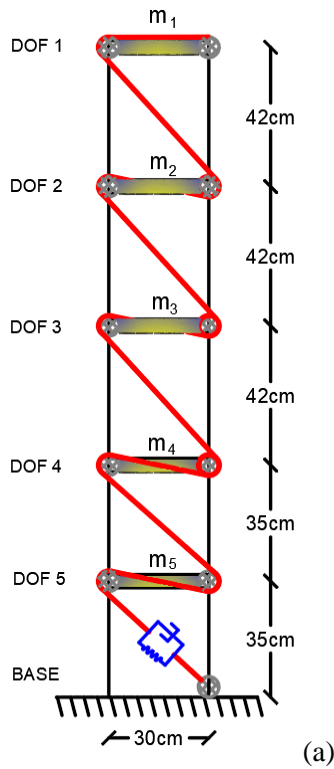


Fig. 1 – Experimental setup of the small-scale five-story shear building on the shake table. (a) schematic elevation, (b) photograph of the experiment

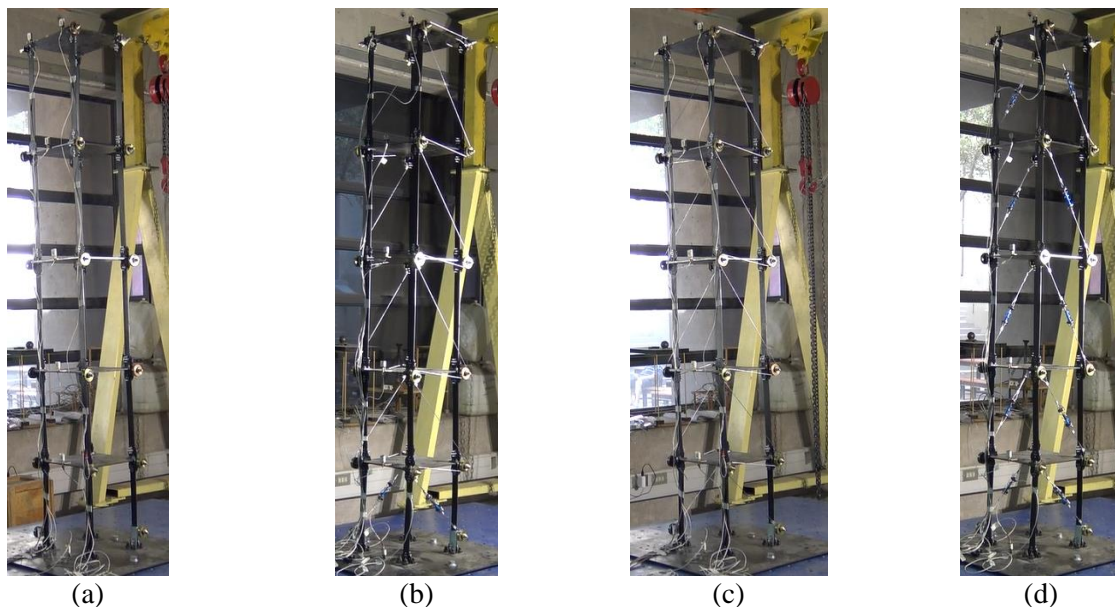


Fig. 2 – Testing configurations of the structure for seismic and pull-back tests: (a) Configuration A: the reference structure (without spring, damper, or cable), (b) Configuration B: structure with spring-dampers in series with a cable, (c) Configuration C: structure with the cable, (d) Configuration D: structure with dampers at every story



3. Results and discussion

3.1 Configuration A: the reference structure

The Deterministic Stochastic subspace Identification (DSI) method [7] is used to estimate the dynamic properties of the reference structure (Fig. 2a). Fig. 3 shows the stabilization diagram and the mode shapes that were identified using the input-output data recorded during the seismic test. Similitude criteria of 1% for frequency, 5% for damping ratios, and 2% for Modal Assurance Criterion (MAC) are considered assuming a model order from 2 to 50 (Allemang and Brown [8]). Note that the sum of the normalized mode shapes $\tilde{\phi} = \phi \cdot (\phi^T \cdot \mathbf{M} \cdot \mathbf{r}) / (\phi^T \cdot \mathbf{M} \cdot \phi)$ identified by using the DSI method is almost equal to the seismic influence vector (i.e., a vector of ones). The fact that the sum of the normalized mode shapes is not precisely equal to a unit vector is because of errors involved in the estimation of the mode shape and inaccuracy in the assumed mass matrix. In Fig. 3b are shown the normalized mode shapes, natural frequencies, and equivalent damping ratios for the five modes identified using DSI.

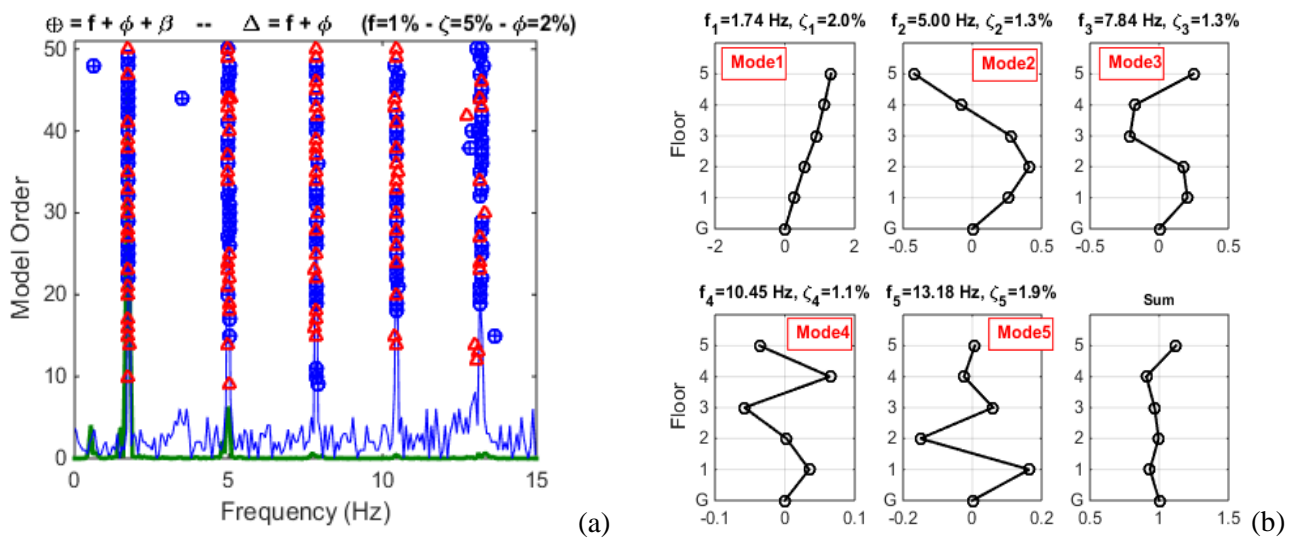


Fig. 3 – System identification results for the structure in Configuration A using the data recorded during the seismic test (a) Stabilization diagram and (b) normalized mode shapes (DSI method)

Hernandez et al. [6] have been presented a novel approach that was called Mod- ζ (var) that allows estimating the time-variant damping ratios and mode shapes from experimental data based on the natural frequencies (time-variant or time-invariant) that are computed from another method. That is, damping ratios and mode shape are obtained to adjust the theoretical response to the measured response by using a Least-Square (LS) Output-error method in the time domain by small-window of data. Fig. 4a shows the Short Time Transfer Function (STTF)[5] computed as the spectral ratio in the frequency domain between the absolute acceleration measured at the roof of the building (DOF1 according to Fig. 1a) and the measured base acceleration for the reference structure by using small windows of data (using a Hanning window of 5.0 seconds overlapped every 2.5 seconds to compute the discrete transfer function of the input and output signals in order to compute the STTF). It is worth noting that the natural frequencies do not change significantly with time during the seismic test, and they are in good agreement with the values identified by using the DSI method (Fig. 3).

Based on the fact that the STTF plot evidences that natural frequencies for the reference structure are practically invariant with time, the Mod- ζ (var) [6] approach is applied assuming constant natural frequencies and equal to values that were identified by using the DSI method (values indicated in the Fig. 3). Additionally, the normalized mode shapes and damping ratios estimated from the DSI method were used as initial values when the Mod- ζ (var) approach was applied. Fig. 5 compares the experimental absolute acceleration time-histories at the different levels of the structure with the corresponding time-histories



computed by using the Mod- $\zeta(\text{var})$ method [6]. An excellent agreement is observed with normalized root mean square errors (NRMSE) higher than 0.53 for all DOFs. The differences between the model-predicted responses and the experimental data could be attributed to external noise and small variations of the natural frequencies of the structure during the seismic test. Fig. 4b shows the STTF obtained from the Mod- $\zeta(\text{var})$ model-predicted absolute acceleration at the roof of the building (DOF1) and the measured base record (used as seismic input for the Mod- $\zeta(\text{var})$ approach).

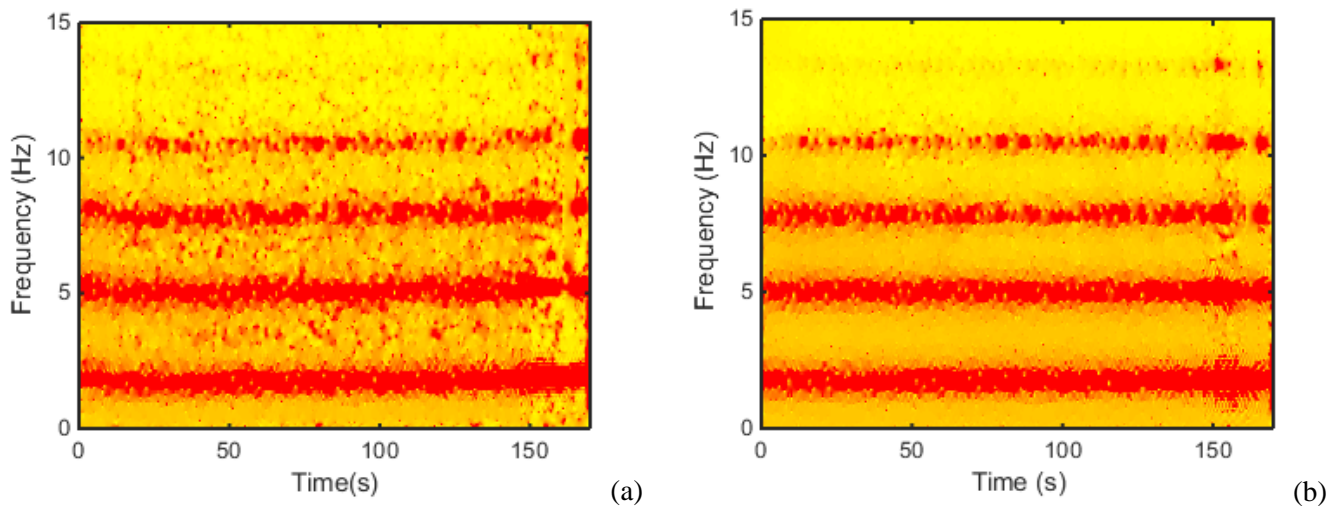


Fig. 4 – Short time transfer function (STTF) between roof and base levels for Configuration A: (a) experimental data, (b) Mod- $\zeta(\text{var})$ model-predicted response

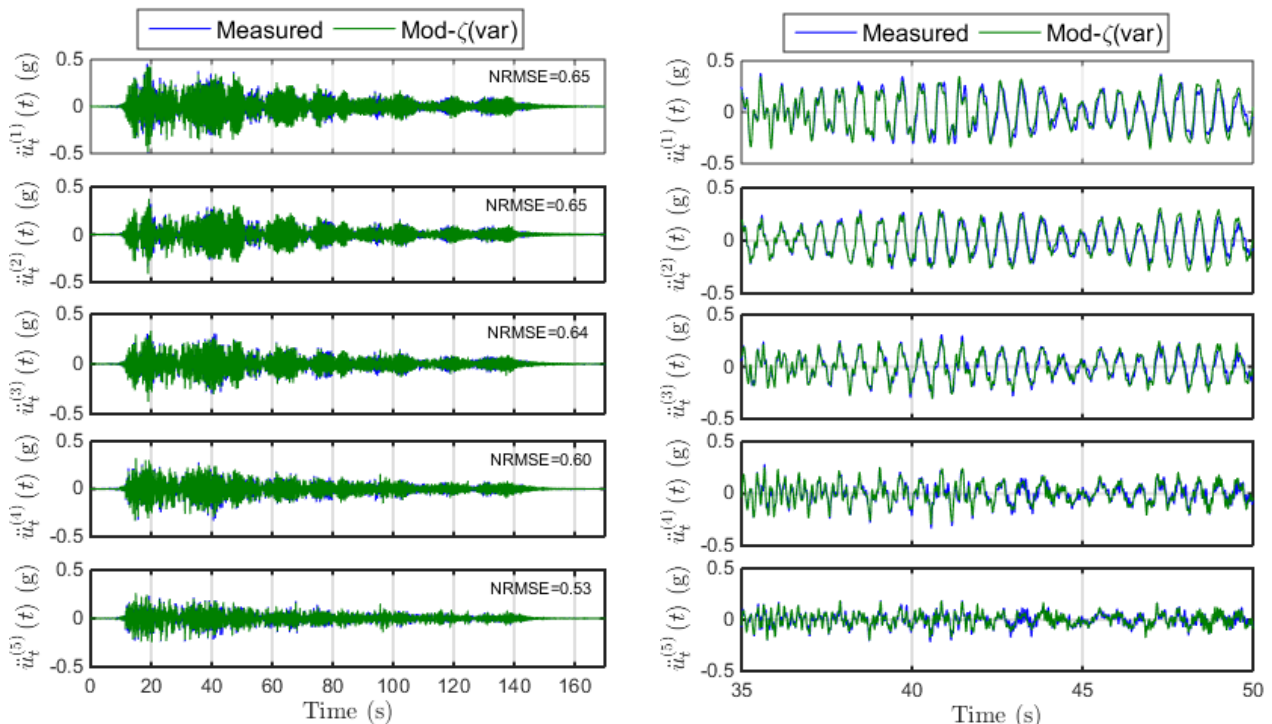


Fig. 5 – Measured and model-predicted (Mod- $\zeta(\text{var})$ method) absolute acceleration time histories at the different levels of the structure for Configuration A. (a) entire record, (b) zoom of the strong motion part

Fig. 6 shows the time-variant damping ratios obtained of the structure by using the proposed Mod- $\zeta(\text{var})$ approach [6]. Additionally, Fig. 6 shows in dashed red lines, the constant damping ratios estimated using the DSI method. It is observed that the computed time-variant damping ratios slightly varied during the



time, and their values are similar to those identified by using the DSI method. The damping ratios identified for the reference structure are low and average for steel structure without nonstructural components, i.e., damping ratios between 0.5% and 2.0% for all structural modes. Note that the damping ratios estimated at the beginning and at the end of the seismic test show very similar values, implying that the structure returned to its initial condition.

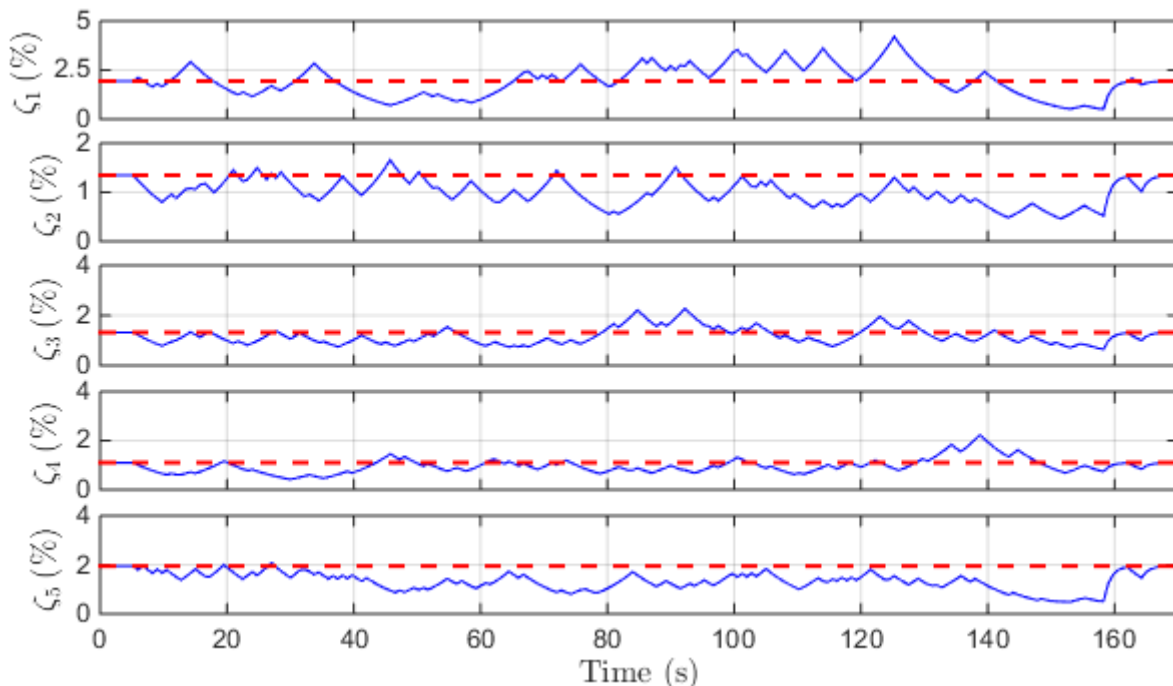


Fig. 6 – Time-variant modal damping ratios for Configuration A

3.2 Configuration B: Structure with a spring-damper energy dissipation device in series with a cable throughout the entire structure

Configuration B corresponds to the five-story building with the proposed system that means all floors of the building are connected with a cable by using a special arrange of pulleys in order to concentrate the inter-story deformations in just one damper-spring device (see Fig. 1 and Fig. 2b). Fig. 7 shows the STTF computed from the spectral ratio between the absolute acceleration of the roof and the base level of the building. The panel on the left-hand side shows the results from the experimental data, while the panel on the right-hand side from the model-predicted response that was obtained by using the Mod- ζ (var) approach [6]. The STTF related to Configuration B evidences that the structure experiences a significant variation of its natural frequencies during the time, i.e., it was related to a non-linear response. For example, the first natural frequency is 4.48 Hz at the beginning and at the end of the seismic test, but it decreases to a minimum value of 2.47 Hz during the strong motion phase (at about 18s). The time-variant frequencies of the structure can be estimated from the STTF plots obtained for all the measured responses. Therefore, smooth time-variant frequencies curves were obtained manually by local inspection of these STTF plots. The time-variant natural frequencies of the first four modes are shown with continuous lines associated with blue, green, red, and cyan colors in Fig. 7. It can be observed that these curves are the same for the experimental and the model-predicted plots since they are used by the Mod- ζ (var) approach [6].

Table 1 shows a summary of the natural frequencies identified for all configurations discussed in this research. In particular, Table 1 shows the initial (or final) natural frequencies that were estimated for Configuration B and its minimum value during the time (identified by using the STTF method). It can be observed that Configuration B, which also applied to configurations C and D, displays a significant variation of its natural frequencies during the strong motion phase in comparison to its initial (or final) values, i.e., it is



observed a reduction between 55-76% of their initial values. Therefore, the natural frequencies were rapidly reduced as soon as the shake table started to move, and they were rapidly recovered when the shake table stopped to move. Moreover, the natural frequencies exhibited by all structural modes of Configuration B (C and D) were higher than natural frequencies obtained for the reference structure (Configuration A), i.e., their minimum values were 128-142% greater than values obtained for Configuration A. These results indicate that the cable-damper system adds stiffness to the structure.

Table 1 – Summary of natural frequencies values and ratios obtained for different structural configurations

Mode	Freq.	Ini. Freq.	Min. Freq.	$\frac{f_m^{(B)}}{f_0^{(B)}}$	$\frac{f_m^{(B)}}{f^{(A)}}$	Min. Freq.	$\frac{f_m^{(C)}}{f^{(A)}}$	Min. Freq.	$\frac{f_m^{(D)}}{f^{(A)}}$
	Conf. A	Conf. B	Conf. B			Conf. C		Conf. D	
	$f^{(A)}$ (Hz)	$f_0^{(B)}$ (Hz)	$f_m^{(B)}$ (Hz)	(%)	(%)	$f_m^{(C)}$ (Hz)	(%)	$f_m^{(D)}$ (Hz)	(%)
1	1.74	4.48	2.47	55.1	142.0	2.41	138.5	2.21	127.0
2	5.00	11.55	7.35	63.6	147.0	6.39	127.8	7.12	142.4
3	7.84	16.66	10.04	60.3	128.1	9.01	114.9	-	-
4	10.45	19.03	14.42	75.8	138.0	19.36	185.3	-	-

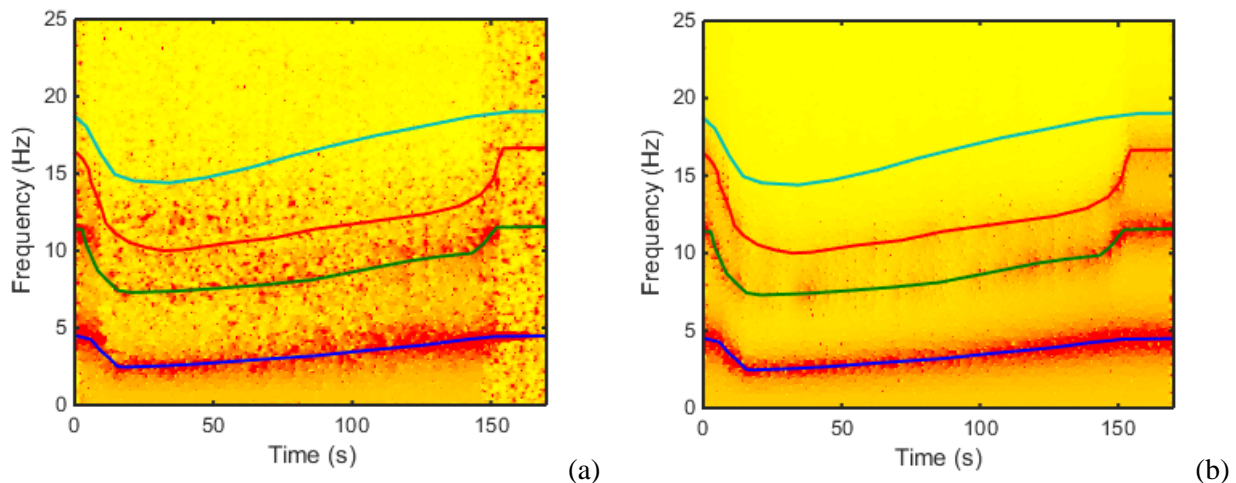


Fig. 7 – Short time transfer function (STTF) between roof and base levels for Configuration B: (a) experimental data, (b) Mod- ζ (var) model-predicted response

The Mod- ζ (var) approach [6] was used to compute the model-predicted response for Configuration B at the different levels of the structure based on the identified time-varying natural frequencies that were obtained from the STTF plot (Fig. 7). Fig. 8 shows the comparison of the measured and model-predicted absolute acceleration time histories for all DOFs by using only the first three normalized modes, which match closely with each other (with NRMSE errors higher than 0.49 for all DOFs). In this context, other higher frequency modes were not employed because they are difficult to distinguish in the STTF plot because of their evident high damping ratios (i.e., they do not play a significant role in the dynamic response).

The DSI method was used to estimate the initial mode shapes and initial damping ratios for the first three modes taking a window of input/output data during the first 1.7 seconds (before the strong motion phase). The estimated damping ratios associated with this initial window of data were 1.86%, 3.57%, and 5.55% for the first three modes, respectively. These values are shown with dashed red lines in Fig. 9. Similarly, Fig. 9 shows the time-variant damping ratios estimated by using the Mod- ζ (var) approach [6]. Note that the damping ratios obtained for configuration B are ostensibly high. In particular, the first mode exhibits a damping ratio ranging from 10% to 17% during the strong motion phase, while the second and



third modes are in the range of 10–20% and 5–12%, respectively. All these values are significantly higher than those estimated for the reference structure in Configuration A (indicated in Fig. 3 and Fig. 6). Thus, it is evidenced that the proposed system can reduce the seismic response by providing additional energy dissipation capabilities for all structural modes. Note that the identified natural frequencies (Fig. 7) and damping ratios (Fig. 9) show identical initial and final values (i.e., at the beginning and end of the seismic excitation), implying that the structure returns to its initial state, i.e., the system has experienced a non-linear elastic behavior.

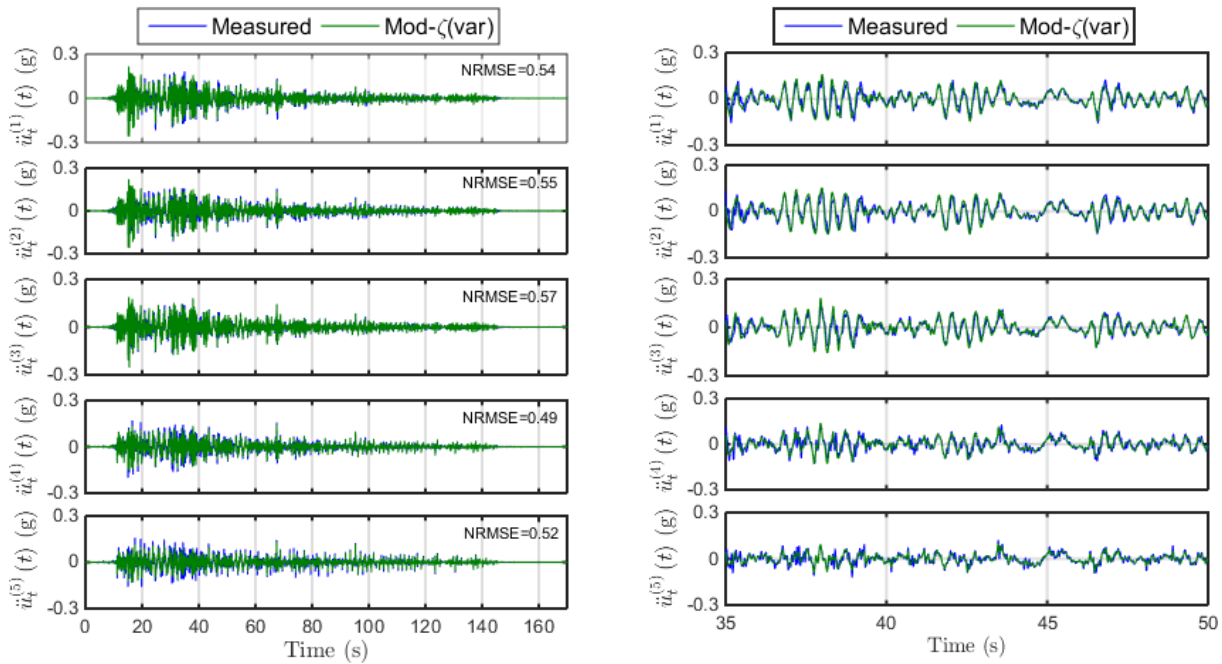


Fig. 8 – Measured and model-predicted (Mod- ζ (var) method) absolute acceleration time-histories at the different levels of the structure for Configuration B. (a) entire record, (b) zoom of the strong motion part

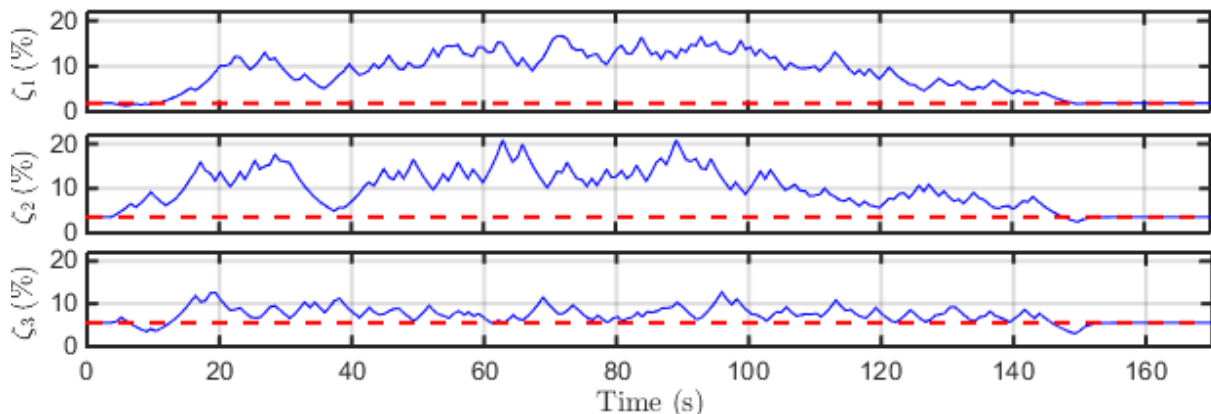


Fig. 9 – Time-variant modal damping ratios for Configuration B

3.3 Configuration C: Structure with the cable only, Configuration D: the structure with dampers on each story

Fig. 10 shows the STTF plots that were obtained from the frequency ratio between the top floor of the building (DOF 1) and the base (using the model-predicted response that was computed by using the Mod- ζ (var) described in Appendix A) for structure Configurations C and D. It can be observed that both configurations have evidenced a significant variation of their natural frequencies during the time. In



particular, Configuration C (only the cable) showed slightly lower frequencies than that for Configuration B (Fig. 7), which could be attributed to the slightly smaller initial pretension of the cable (with and without the damper-spring system). It is important to have in mind that the pretension of the cable has been idealistically controlled by imposing that the cable had emitted the same sound frequency when it was subjected to prestress before the seismic tests (using a guitar tuner). Similarly, it is also drawn that Configuration D showed higher natural frequencies than Configuration A, B, and C, which implies that the system with multiples damper-spring on every floor adds more stiffness than the configurations B or C. Fig. 11 shows the comparison between the model-predicted response by using the Mod- $\zeta(\text{var})$ approach and absolute experimental acceleration data for Configuration C and D. Both adjustments show an excellent match between model-predicted and experimental data with RMSE errors higher than 0.44 for all channels.

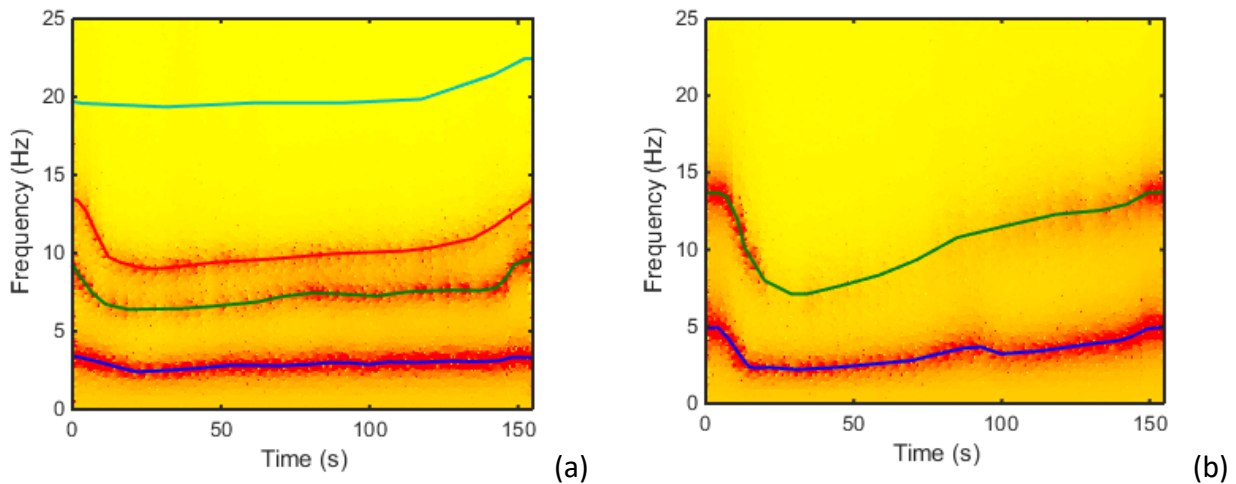


Fig. 10 – Short time transfer function (STTF) between roof and base levels for Mod- $\zeta(\text{var})$ model-predicted response: (a) Configurations, (b) Configuration D

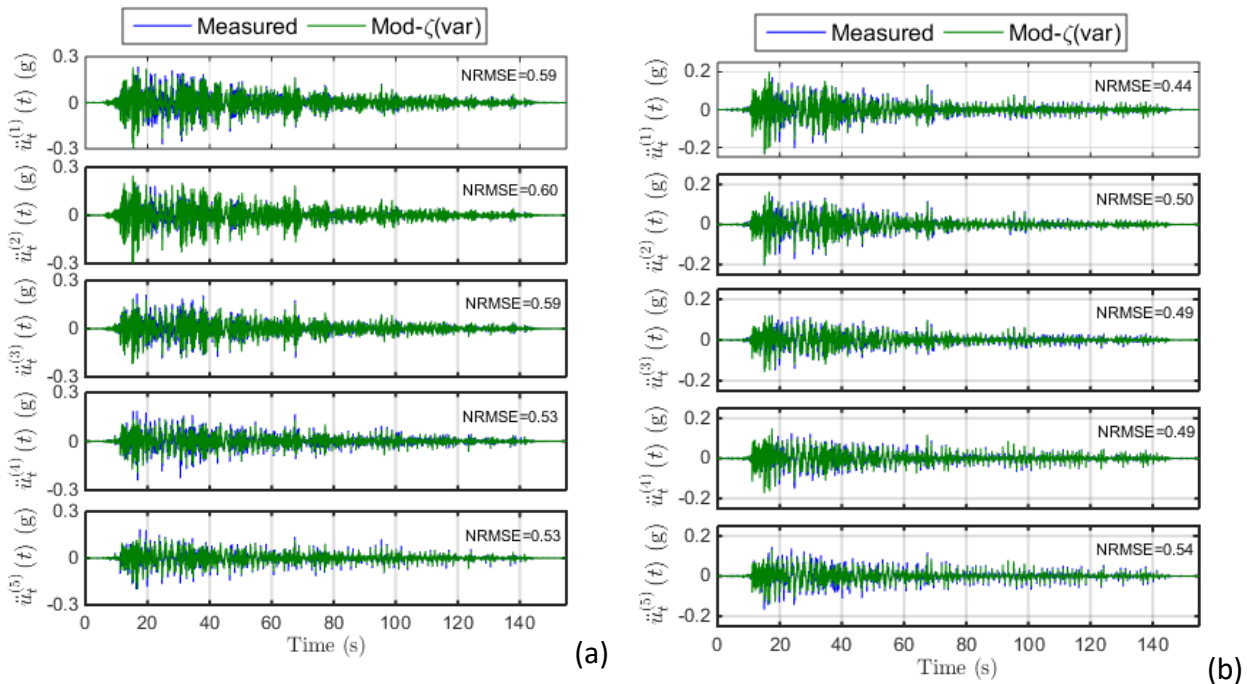


Fig. 11 – Measured and model-predicted (Mod- $\zeta(\text{var})$ method) absolute acceleration time histories at the different levels of the structure. (a) Configuration C. (b) Configuration D



Fig. 12 shows the time-variant damping ratios for Configurations B, C, and D (using a synchronized time). Configuration B was adjusted by using three modes and Configuration D by using only two modes. The latter occurs because of the low response participation related to the omitted modes due to their high damping ratios. It can be concluded that Configuration C pulleys (without the damper-spring dissipator) provides significant damping ratios and comparable to the dissipation provided by Configuration B. This indicates that the pulley-cable system by itself was able to dissipate the main part of the seismic energy due to friction between the cable and pulleys, and the intrinsic viscous damping that occurred inside the pulley mechanisms. Configuration B and C show almost identical damping ratios during the first part of the strong motion. However, Configuration B shows significant damping ratio values during the entire seismic test, which were consequently higher than damping ratios obtained for Configuration C during the long-term phase of the seismic event. This indicates that the initial impulsive response is initially dissipated by the cable-pulley system, and the damper-spring system only played a significant role during the last part of the strong motion because it continues mitigating the seismic response, providing a high dissipation during the entire seismic event. On the other hand, Configuration D (dampers on all floors) also showed a significant seismic energy dissipation during the entire seismic event, which was slightly higher than the dissipation provided by Configuration B. This is because dampers were placed on all floors. In agreement with previous observations, Configurations C and D showed the capability to return to its original state, because their natural frequencies and damping ratios started and finished with almost the same values, indicating that these configurations were also elastic.

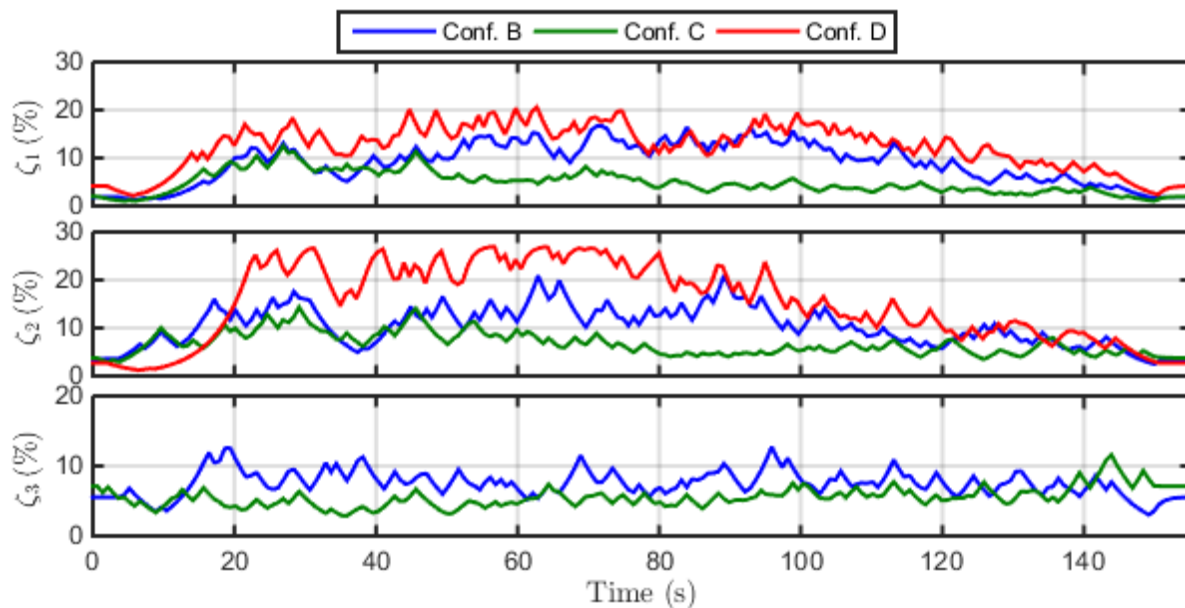


Fig. 12 – Time-variant modal damping ratios for Configurations B, C, and D

Fig. 13 shows the peak inter-story shear forces and the peak inter-story drift of each story for all the structural configurations tested above. It can be observed that Configuration B can reduce the peak shear inter-story forces on approximately 40% (i.e., 60% of their values) and inter-story drifts on 30% in comparison to Configuration A. Similarly, Configuration B reduces peak seismic demands on a fraction slightly higher than Configuration C (structure with only the cable). It indicates that the peak values that are observed during the initial phase of the strong motion (impulsive part) were almost identical, which leads to conclude that both Configurations B and C provide a similar efficiency in terms of reduction of peak seismic demands. It can be concluded that the cable-pulley system was the primary seismic energy dissipation system (at least during the initial phase of the strong motion), and the damper-spring has played a secondary role in the reduction of these quantities. In the meanwhile, it can be observed that Configuration D (dampers placed on all floors) provides a slightly higher reduction of the seismic demand in comparison to Configuration B or C.

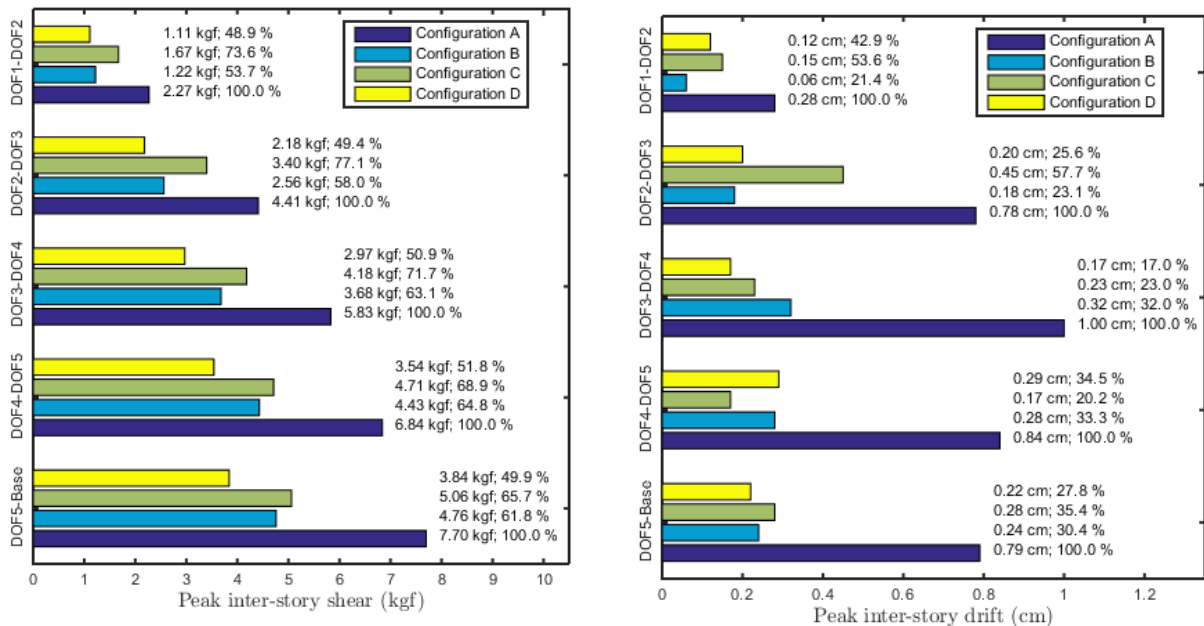


Fig. 13 – Inter-story shear force and inter-story drift reductions for all configurations

4. Conclusions

A novel system that uses a unique energy dissipation device in series with a cable through the entire structure has been tested in a shake table in order to verify that the cable can concentrate the inter-story deformation in the damper-spring device. As a result, it has been observed that the proposed system was able to provide high damping ratios for all structural modes ($>10\%$) during strong seismic motions. The high seismic energy dissipation provided by the proposed system has ostensibly reduced the seismic demand in comparison to Configuration A (the reference structure), mitigating the inter-story drifts in 70% approximately.

It was observed that structural configurations that have a cable system (Configuration B, C, and D) had experienced a high nonlinear response. This nonlinear behavior was evidenced by the high variations of their natural frequencies (and damping ratios) during the time. The structural configurations after and before the strong ground motion have shown the same dynamic properties indicating the structures were able to come back to their initial states. Structural configurations that have a cable have increased the stiffness of the structure; however, during the strong ground motion, the natural frequencies were rapidly reduced to values that were closer to the frequencies that are observed for the structure without energy dissipation devices (Configuration A).

During the shake table tests, it was observed that the proposed system had provided a seismic energy dissipation that is slightly lower than the provided by placing a damper on every floor. It is evident that the proposed system is highly efficient, taking into account that the proposed system requires to use a reduced number of energy dissipation devices (reducing costs), and it is also less invasive with respect to architecture point of view.

The main seismic energy dissipation was provided by the cable-pulleys interaction, and the damper-spring device has played a secondary role. However, it was also observed that the damper-spring system provided higher damping ratios during the long-term of the strong seismic motion.



5. Acknowledgments

The authors acknowledge the financial support from the Chilean National Commission for Scientific and Technological Research (CONICYT) through the research grant FONDEF ID 18I10103. The authors also acknowledge the support provided by Professor Pedro Soto from the University of Chile.

6. References

- [1] Fu Y, Kasai K (1998):Comparative Study using Viscoelastic and Viscous Dampers. *J Struct Eng*, **124** (5), 513–22.
- [2] Lagos R, Kupfer M, Lindenberg J, Bonelli P, Bonelli P, Saragoni R, et al. (2012):Seismic Performance of High-rise Concrete Buildings in Chile. *Int J High-Rise Build*, **1** (3), 181–94.
- [3] Takewaki I (1997):Optimal Damper Placement for Minimum Transfer. *Earthq Eng Struct Dyn*, **26**, 1113–24.
- [4] Xu ZD, Zhao HT, Li AQ (2004):Optimal analysis and experimental study on structures with viscoelastic dampers. *J Sound Vib*, **273** (3), 607–18.
- [5] Hernández F, Días P, Ochoa-Cornejo F, Astroza R Time variant system identification of superstructures of base-isolated buildings (working paper). (2019).
- [6] Hernández F, Astroza R, Beltrán JF, Zhang H, Mercado V A novel cable-pulley spring-damper energy dissipation system for buildings (working paper). (2020).
- [7] Van Overschee P, De Moor B Subspace Identification for Linear System: Theory - Implementation - Applications. Kluwere Academic Publishers; (1996).
- [8] Allemang RJ, Brown DL (1982):A correlation coefficient for modal vector analysis. *First Int Modal Anal Conf*, 110–6.
- [9] Cohen L (1994):Time Frequency Analysis - Theory and Applications.
- [10] Huang NE, Shen Z, Long SR, Wu MC, Shih HH, Zheng Q, et al. (1998):The empirical mode decomposition and the Hilbert spectrum for nonlinear and non-stationary time series analysis. *R Soc London*, **454**, 903–95.